

Localized Moments on Rhodium in *Pd-Rh* Alloys*

G. N. RAO, E. MATTHIAS, AND D. A. SHIRLEY

*Department of Chemistry and Lawrence Radiation Laboratory,
University of California, Berkeley, California 94720*

(Received 7 April 1969)

The Knight shifts of ^{100}Rh in very dilute *Pd-Rh* alloys were measured over a temperature range between 4.2 and 1053°K by γ - γ perturbed angular-correlation techniques. The Knight shifts were negative, very large (up to -15%), and strongly temperature-dependent. The Curie-Weiss behavior of the Knight shift and the difference between its temperature dependence in a dilute *Pd-Rh* alloy and in pure palladium, establish the existence of a local moment on the rhodium atom. From existing susceptibility data, the impurity susceptibility χ_i was calculated. Its temperature dependence is conspicuously different from that of the Knight shift. The partial derivative $\partial K_i(T)/\partial \chi_i(T)$ was used to obtain the apparent core-*d* hyperfine field, $H_{\text{hf}}^{(d)}$. The result is $H_{\text{hf}}^{(d)} \approx -700$ kG for $T > 400^\circ\text{K}$, and $H_{\text{hf}}^{(d)} \approx -43 \pm 1$ kG for $T < 400^\circ\text{K}$. The drastic change in the field at about 400°K indicates that above this temperature the localized moment is concentrated on the Rh atom, while at lower temperatures the polarization of the lattice by the impurity atom seems to be rather long ranged, suggesting the formation of a quasibound state. Knight shifts for ^{100}Rh in Ag and Pt hosts are also reported.

I. INTRODUCTION

THE formation of localized moments on impurity atoms in various metal alloys is well known for solute atoms of the 3*d* transition group.¹ Much less experimental evidence is presently available about localized states on 4*d* atoms in dilute alloy systems. We have studied this question in the *Pd-Rh* alloy system.

The macroscopic properties of this system—susceptibility, resistivity, and specific heat—have been studied previously. The anomalous variation of the susceptibility of *Pd-Rh* alloys with temperature, as well as with rhodium concentration, has been of particular interest.²⁻⁶ The susceptibility maximum in palladium around 85°K led Lidiard³ to assume that an antiferromagnetic state occurs below 85°K, but other experiments do not support this contention. The anomalous peak in susceptibility around 85°K can also be obtained by assuming a special distribution for the density of states near the Fermi level.⁷ No evidence for the existence of a second-order transition was obtained from specific-heat measurements.⁸ Neutron diffraction

experiments⁹ have established that at low temperatures the spontaneous moment per Pd atom must be less than $0.03\mu_B$. NMR experiments showed that the magnetic moment should be several orders of magnitude smaller than the upper limit given from the neutron diffraction experiments.¹⁰ Additional experimental studies on resistivity and thermoelectric power¹¹ as a function of temperature with small impurities of rhodium would be helpful in interpreting the susceptibility data for *Pd-Rh* alloys.

The present Knight-shift studies were undertaken to see whether or not a localized moment is formed on the rhodium atom in a palladium matrix. Usually, a localized moment is detected through magnetic moment measurements, as well as through the temperature dependence of incremental changes in susceptibility, resistivity, specific heat, and thermoelectric power resulting from the addition of small concentrations of the impurity to the host metal. In the work reported here, we tried to establish the existence of a local moment by studying the temperature dependence of the Knight shift of the impurity nucleus. We used the method of perturbed γ - γ angular correlations, since the decay of ^{100}Rh is a favorable case¹² for this type of measurement. Besides the advantage of an extremely high sensitivity, this method is sufficiently accurate to measure the change of the Knight shift of ^{100}Rh in very dilute *Pd-Rh* alloys.

The angular correlation method is described in Sec. II. Data analysis is treated in Sec. III. Results are given in Sec. IV. In Sec. V, the Knight-shift data are compared with the impurity susceptibility and conclusions are drawn about the localized state.

Naturforsch. **11A**, 955 (1956); D. Clusius and L. Schachinger, *ibid.* **2A**, 90 (1947).

⁹ S. C. Abrahams, *Phys. Chem. Solids* **24**, 589 (1963).

¹⁰ J. A. Seitchik, A. C. Gossard, and V. Jaccarino, *Phys. Rev.* **136**, A1119 (1964).

¹¹ T. Ricker and R. Luck, *Z. Metallk.* **56**, 799 (1965).

¹² E. Matthias, D. A. Shirley, J. S. Evans, and R. A. Naumann, *Phys. Rev.* **140**, B264 (1965).

* A preliminary report of this work was reported at the Solid State Physics section of the American Physical Society Meeting at Berkeley. [*Bull. Am. Phys. Soc.* **13**, 409 (1968)]. This work was done under the auspices of the U. S. Atomic Energy Commission.

¹ For a recent comprehensive review see M. D. Daybell and W. A. Steyert, *Rev. Mod. Phys.* **40**, 380 (1968).

² F. E. Hoare and J. C. Matthews, *Proc. Roy. Soc. (London)* **A212**, 137 (1952); D. Budworth, F. E. Hoare, and J. Preston, *ibid.* **A257**, 250 (1960); R. Doelo, S. Foner, and A. Narath, *Bull. Am. Phys. Soc.* **13**, 363 (1968).

³ A. B. Lidiard, *Proc. Roy. Soc. (London)* **A227**, 161 (1954).

⁴ J. A. Seitchik, V. Jaccarino, and J. H. Wernick, *Phys. Rev.* **138**, A148 (1965).

⁵ A. J. Manuel and J. M. P. St. Quinton, *Proc. Roy. Soc. (London)* **A273**, 412 (1963).

⁶ V. E. Vogt, E. Oehler, and W. Treutmann, *Ann. Physik* **18**, 168 (1966).

⁷ E. W. Elcock, P. Rhodes, and A. Teviotdale, *Proc. Roy. Soc. (London)* **A221**, 53 (1954).

⁸ J. Crangle and T. F. Smith, *Phys. Rev. Letters* **9**, 86 (1962); B. M. Boerstoeel, F. J. du Chantener, and G. J. Vandenberg, in *Proceedings of the Ninth International Conference on Low-Temperature Physics, Columbus, 1964* (Plenum Press, Inc., New York, 1965), Part B, p. 1071; W. Eichenhauer and L. Schäfer, *Z.*

II. EXPERIMENTAL METHOD

Let us consider a γ - γ cascade, where the nucleus in an excited state A decays to the intermediate state B by the emission of γ_1 , and then to the final state C by the emission of γ_2 . If the nuclei are initially oriented at random, i.e., if all the magnetic substates have equal population, the γ radiation emitted from the nuclei will have an isotropic intensity distribution. In a γ - γ coincidence experiment, a system of oriented nuclei is prepared by choosing those nuclei in the intermediate state that have emitted γ radiation in a fixed direction \mathbf{k}_1 . Because of the multipole character of the γ radiation, γ_2 quanta emitted in the direction \mathbf{k}_2 will have a non-isotropic intensity distribution with respect to \mathbf{k}_1 . If there are no extranuclear perturbations acting on the intermediate state B , this intensity distribution can be expressed in terms of the Legendre polynomials¹³

$$W(\theta) = \sum_{\lambda \text{ even}} A_{\lambda}(1)A_{\lambda}(2)P_{\lambda}(\cos\theta), \quad (1)$$

where $\theta = \angle(\mathbf{k}_1, \mathbf{k}_2)$. The coefficients $A_{\lambda}(1)$ and $A_{\lambda}(2)$ depend on the spins and multiplicities of the transitions γ_1 and γ_2 , and are tabulated in Ref. 14.

A magnetic field \mathbf{H}' at the nucleus interacts with the static magnetic dipole moment \mathbf{u} of the intermediate state B , during the time interval between the formation of this state ($t=0$) and the emission of γ_2 at time t . The interaction Hamiltonian has the form

$$\mathcal{H} = -\mathbf{u} \cdot \mathbf{H}'. \quad (2)$$

If the magnetic field \mathbf{H}' is perpendicular to the plane containing \mathbf{k}_1 and \mathbf{k}_2 , the angular correlation pattern $W(\mathbf{k}_1, \mathbf{k}_2)$ simply rotates around the \mathbf{H}' axis with the Larmor precession frequency

$$\omega_L = -gH'(\mu_N/\hbar). \quad (3)$$

In this case, the perturbed angular correlation (PAC) can again be expressed in terms of Legendre polynomials

$$W_1(\theta, t) = \sum_{\lambda} A_{\lambda}(1)A_{\lambda}(2)P_{\lambda}[\cos(\theta - \omega_L t)]. \quad (4)$$

Time t and angle θ are now equivalent, and by keeping the detectors at a fixed angle θ_0 , one can observe periodic intensity modulations in the time spectrum of the coincidences (a typical example is shown in Fig. 1). From the periodicity of those modulations, the product gH' can be extracted.

The PAC technique provides an excellent tool to sense microscopically the magnetism associated with an impurity atom in a metallic host lattice. The rotation

of the angular correlation pattern yields the effective magnetic field

$$H' = H_0(1 \pm K_i), \quad (5)$$

where H_0 is the applied field and K_i , the impurity Knight shift

$$K_i = \Delta H_i/H_0 = (8\pi/3)\langle |\psi(0)|^2 \rangle_{\mathcal{E}F} \chi_i. \quad (6)$$

This method is many orders of magnitude more sensitive than conventional NMR. Unlike the Mössbauer effect, the PAC technique can be used at any temperature, and is, therefore, well suited for studying the temperature dependence of Knight shifts.

To study very dilute Pd -Rh alloys, we used the angular correlation of the 84-75-keV cascade in ¹⁰⁰Rh, populated in the decay of 4-day ¹⁰⁰Pd (Fig. 2).¹⁵ The anisotropy of this correlation is about +30%.¹² The intermediate state of this cascade has a half-life of $T_{1/2} = 235$ nsec, and a g factor of $g = +2.151$.

¹⁰⁰Pd was produced by ($p, 4n$) reaction on a target of pure rhodium metal (100% ¹⁰³Rh) foil, with an incident proton energy of 45 MeV, at the Berkeley 88-in. cyclotron. Chemically-separated¹⁶ carrier-free ¹⁰⁰Pd was electroplated on pure (99.5-99.997%) palladium foil, which was then melted in an induction furnace, in vacuum, after flushing several times with argon. The molten alloys were kept in the liquid state for at least 10 min, so that the radioactive palladium dissolved uniformly into the host metal, and thereafter they were gradually cooled down to room temperature over about 12 h. The resulting shiny alloys were rolled and annealed in the induction furnace from 12 to 20 h at 950°C and cooled gradually. The source dimensions were approximately 0.25 mm² with a thickness of about 20 000 Å.

Two thin-window Ge(Li) diodes specially made for fast-timing work were used for detecting the 84- and 75-keV γ rays. Fast and slow pulses from the germanium detectors were fed into the time- and energy-selecting channels, respectively (Fig. 3). Each fast-timing circuit consisted of three 1-nsec amplifiers followed by a 100-Mc/sec interface discriminator. Outputs from the interface discriminators served as the start and stop pulses for an "Eldorado" time-interval counter, model 793, which measures the delay between the two γ rays to 1-nsec accuracy. This digitized time information was dumped through an interface onto IBM-compatible magnetic tape via a Kennedy 1500/5 incremental tape unit. The start and stop pulses were energy gated in the conventional way. In parallel to the digital counter computer, data were also taken with an analog time-to-height converter (adjusted for a range of 1.6 μ sec) and a multichannel analyzer in the coincidence mode (see Fig. 3). The multichannel analyzer was calibrated with the help of an "Eldorado" digital delay pulse generator,

¹³ R. M. Steffen and H. Frauenfelder, in *Perturbed Angular Correlations*, edited by E. Karlsson, E. Matthias, and K. Siegbahn (North-Holland Publishing Co., Amsterdam, 1964), Chap. I; H. Frauenfelder and R. M. Steffen, in *Alpha-, Beta-, and Gamma-Ray Spectroscopy*, edited by K. Siegbahn (North-Holland Publishing Co., Amsterdam, 1965), Vol. 2, Chap. 19A.

¹⁴ M. Ferentz and N. Rosenzweig, Argonne National Laboratory Report No. ANL-5324, 1954 (unpublished).

¹⁵ J. S. Evans and R. Naumann, Phys. Rev. **138**, B1017 (1965).

¹⁶ J. S. Evans, E. Kashy, R. A. Naumann, and R. F. Petry, Phys. Rev. **138**, B9 (1965).

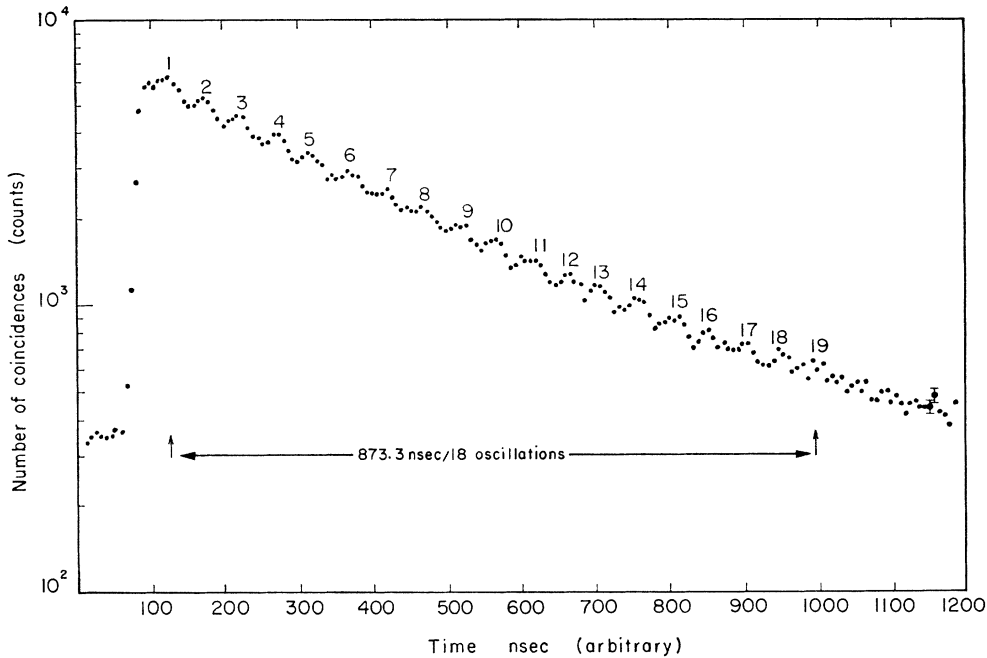


FIG. 1. Multichannel time spectrum of ^{100}Rh in silver, at room temperature, in an external magnetic field of 6250 G. The data have not been corrected for background.

model 610, which puts out pulses with an adjustable delay of 1-999 999 nsec between start and stop pulses.

III. DATA ANALYSIS

In the case of the 84-75-keV cascade of ^{100}Rh with spin sequence $1+ \rightarrow 2+ \rightarrow 1-$, the summation index λ is limited to $\lambda=0, 2$, and the time dependence of $W(\theta_0, t)$ appears as a sinusoidal modulation. The total time spectrum of the coincidences (see Fig. 1) can be

described by a six-parameter equation that takes into account exponential decay, background and phase of the rotation:

$$I(t) = a + be^{-t/\tau} [1 + c \sin(2\omega t + \phi)]. \quad (7)$$

The amplitude of the modulation is related to the conventional angular correlation coefficients in Eq. (4):

$$c = \frac{3}{4} A_2(1) A_2(2) / [1 + \frac{1}{4} A_2(1) A_2(2)]. \quad (8)$$

Both Fourier analysis and autocorrelation techniques were used to extract the frequency of the Larmor precession from the data.¹⁷ The sin, cos, and absolute

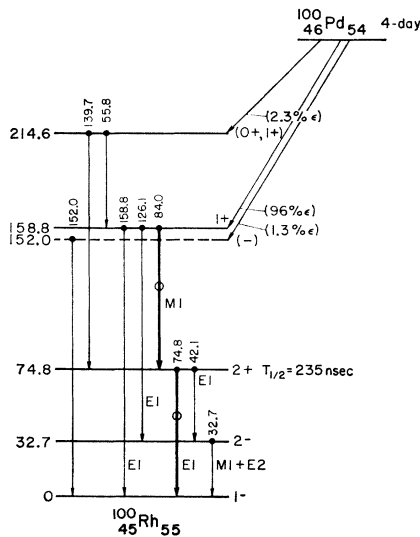


FIG. 2. Decay scheme of ^{100}Pd .

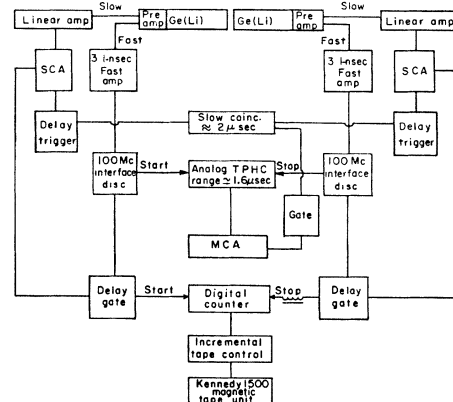


FIG. 3. Block diagram of the electronics.

¹⁷ E. Matthias and D. A. Shirley, Nucl. Instr. Methods 45, 309 (1966).

Fourier transforms were calculated from the equations

$$\begin{aligned} A(\omega) &= \int_0^{T_{\max}} I(t) \sin \omega t dt, \\ B(\omega) &= \int_0^{T_{\max}} I(t) \cos \omega t dt, \\ F(\omega) &= [A^2(\omega) + B^2(\omega)]^{1/2}. \end{aligned} \quad (9)$$

It should be noted that only the absolute transform $F(\omega)$ can be used for frequency determination. To evaluate ω_L from the data, the typical procedure is: The number of coincidences in 1–1000 nsec are picked up from the magnetic tape and the data are fitted with Eq. (7). The best values for background, exponential, and phase are then used for calculating the Fourier transforms [Eq. (9)]. A typical plot of the sin, cos, and absolute transforms for Ag-Rh at room temperature are shown in Fig. 4. Multichannel data can be analyzed in the same way, and the upper parts of Figs. 5 and 6 represent examples.

By using the autocorrelation function, it is possible to improve the signal-to-noise ratio by more than an order of magnitude compared to the simple Fourier transform.¹⁷ In this technique, the Fourier integral

$$G(\omega) = \int_0^{T_{\max}} \frac{C(T)}{C(0)} \cos \omega T dT \quad (10)$$

contains the autocorrelation function

$$\frac{C(T)}{C(0)} = \frac{\langle [W(t) - \bar{W}][W(t+T) - \bar{W}] \rangle_{\text{av}}}{\langle [W(t) - \bar{W}][W(t) - \bar{W}] \rangle_{\text{av}}}, \quad (11)$$

where T is the time lag at which the data are correlated.

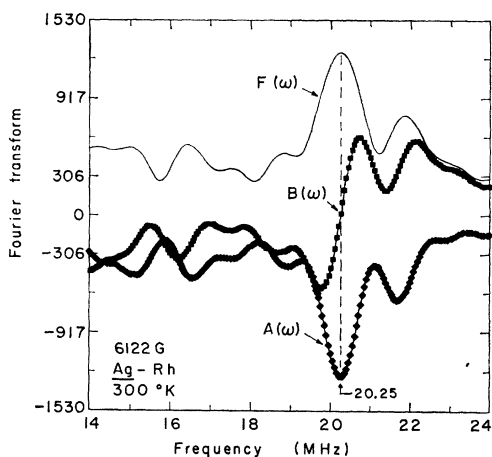


FIG. 4. Sine, cosine, and absolute transforms of the time spectrum for ^{100}Rh in silver, at room temperature, in a magnetic field of 6122 G. The data were recorded with the digital THC.

Typical autocorrelation spectra are shown in the lower parts of Figs. 5 and 6.

IV. RESULTS

The results of our Knight-shift measurements of ^{100}Rh in palladium, silver, and platinum hosts are given in Tables I and II. For the evaluation of the Knight shifts, the g factor of the 75-keV state in ^{100}Rh was taken as +2.151.¹² This value contains a correction for the Knight shift, $K = +0.43\%$, of rhodium nuclei in rhodium metal as reported by Seitchick *et al.*³

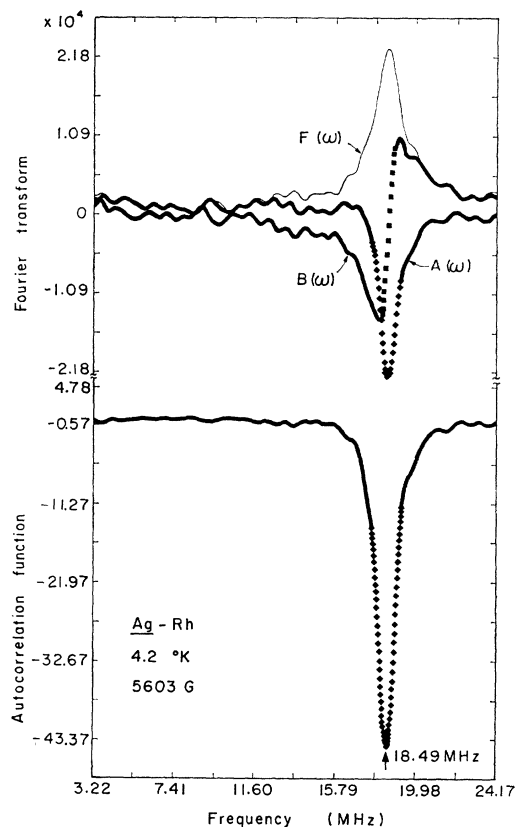


FIG. 5. Fourier transforms (upper part) and autocorrelation function (lower part) of the time spectrum for ^{100}Rh in silver, at 4.2°K, in a magnetic field of 5603 G. Data taken with a multichannel analyzer were used for the analysis.

The quoted error represents mainly the standard deviation of the frequency obtained from fitting Eq. (7) to the data. The magnetic field was measured by proton resonance. To control drifts the proton resonance was checked before, during, and after a measurement. In all cases, the error in the magnetic field was found to be negligible compared to the statistical uncertainty in the frequency. For the digital THC, the time calibration is intrinsically determined by the counting frequency of the time-interval counter, and is accurate to better than 1 nsec over the total range of the counter. When

multichannel data were used for the Fourier analysis, the analog THC was calibrated by a digital delay pulse generator (Eldorado 610) which provided the same accuracy as obtained with the digital THC. This uncertainty in the time calibration was small compared to the standard deviation of the frequency fit. Table III shows the reproducibility and typical errors of three runs made with ^{100}Rh in silver at 300°K.

For all results presented here, impurity-impurity interactions can safely be neglected. All sources were made by electroplating the carrier-free palladium activity on the host metal. After most of the 4-day

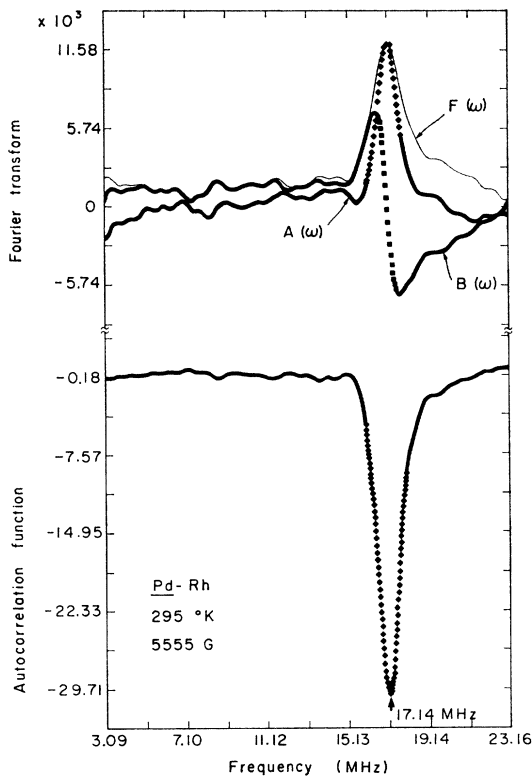


FIG. 6. Fourier transforms (upper part) and autocorrelation function (lower part) of the time spectrum for ^{100}Rh in palladium, at room temperature, in a magnetic field of 5555 G. Multichannel data were used for the analysis.

palladium activity had decayed to rhodium, a spectroscopic analysis of the metallic sources was done in a dc arc: No detectable traces of rhodium lines were observed in the emission spectra. Activation analysis showed that the rhodium concentration is less than 1 part in 10^7 of the host metal. Most of these measurements were repeated with different palladium host purities (99.5, 99.95, and 99.997%), but no detectable changes in the results were observed. This is quite expected, because the effective magnetic field H_{eff} seen by the rhodium nucleus is a *microscopic* property specific to the rhodium atom. By contrast, a macroscopic property such as the total mass susceptibility would be extremely sensitive

TABLE I. Knight-shift data for dilute Pd-Rh alloys obtained at various temperatures. The values given represent weighted averages over several individual runs.

$T(^{\circ}\text{K})$	$g(1+K)$	$-K$
4.2	1.835 (7)	0.147 (3)
77	1.914 (7)	0.120 (4)
195	2.006 (6)	0.067 (3)
295	2.014 (2)	0.064 (2)
373	2.033 (4)	0.055 (3)
503	2.070 (4)	0.038 (3)
803	2.132 (5)	0.009 (3)
1053	2.121 (7)	0.014 (4)

to impurities, especially to paramagnetic impurities at low temperatures.

Aftereffects due to electron-capture decay of the ^{100}Pd activity are not expected to affect the results, since the measurements were performed with metallic sources. In a metal, a hole in the K shell formed after the electron capture should move out to the conduction band and diffuse away in less than 10^{-12} sec, or fast compared to the decay of the 159-keV state from which the 84-keV γ ray emanates, let alone that of the 235-nsec state.

TABLE II. Knight-shift measurements in ^{100}Rh in silver and platinum host metals.

Alloy	Temp. ($^{\circ}\text{K}$)	g factor $g(1+K)$	Knight shift (K)
Ag-Rh	300	2.171 (2)	+0.009 (2)
Ag-Rh	77	2.177 (3)	+0.012 (3)
Ag-Rh	4.2	2.165 (3)	+0.007 (3)
Pt-Rh	300	2.070 (2)	-0.038 (2)

The angular correlation could, in principle, be perturbed by quadrupole interactions. In all measurements presented here, this is unlikely since the host metals used have cubic structure and form solid solutions with the radioactive palladium. The decaying nucleus sees the cubic symmetry of the host metal, and impurity-impurity interactions must be small because of their great dilution. This is verified by the present (see Fig. 1) and previous¹² experiments where no attenuation of the anisotropy was observed within the experimentally measured time range of about 1.2 μsec . The autocorrelation in Figs. 5 and 6 yields a line width very close to the natural width ($2\Delta\nu = 1/\pi\tau = 0.94$ MHz).

TABLE III. Typical errors involved in three runs for ^{100}Rh in silver at room temperature.

Run No.	Magnetic field (G)	Frequency (MHz)	$g(1+K)$	Knight shift (K)
1	6122 (3)	20.27 (3)	2.172 (3)	+0.010 (2)
2	6250 (3)	20.67 (5)	2.169 (5)	+0.008 (3)
3	6250 (3)	20.70 (5)	2.172 (5)	+0.010 (3)
Weighted average			2.171 (2)	+0.009 (1)

This evidence also permits the conclusion that any nuclear relaxation time is much larger than 1 μ sec.

V. DISCUSSION

The Knight shift defined in Eq. (6) is the ratio of the additional magnetic field experienced by the nucleus in a metallic medium compared to the diamagnetic base for a pure metal.¹⁸ It depends on the Fermi electron density at the nucleus, $\langle |\psi(0)|^2 \rangle_{E_F}$ and the total electronic susceptibility χ . We shall not be concerned here with the absolute magnitude of the impurity Knight shift, which in itself is a highly interesting problem.¹⁹ The goal of the present work was to use the temperature dependence of the Knight shift to identify the localized moment formed by a rhodium atom in a palladium matrix.

In the rigid-band model, one assumes that the s and d bands are distinguishable at the Fermi energy (E_F). The density of states at E_F is then just the sum of the s and the d band contributions,

$$N(E_F) = N(E_F)_s + N(E_F)_d. \quad (12)$$

Assuming that the spin-orbit contribution to the susceptibility is small, the total electronic susceptibility in a *pure* metal may be written as²⁰

$$\chi(T) = \chi_P^s + \chi_P^d(T) + \chi_{VV} + \chi_{dia}, \quad (13)$$

where χ_P^s and χ_P^d are the Pauli-spin susceptibilities due to the s - and d -spin electrons, χ_{VV} is the analog of the temperature-independent Van Vleck susceptibility, and χ_{dia} is the diamagnetic susceptibility of the core.

If the spin-orbit interactions may be neglected, the total hyperfine field H_{hf} , experienced by the nucleus in a pure metal, arises from the contact interaction of the conduction-band s electrons, core polarization by the d electrons, and the orbital hyperfine field contribution. In close analogy to the susceptibility, the Knight shift as a function of temperature can be expressed as²⁰

$$K(T) = K_s + K_d(T) + K_{VV} + \delta K_{dia} \quad (14)$$

or

$$K(T) = \alpha_s \chi_P^s + \alpha_d \chi_P^d(T) + K_{VV} + \delta K_{dia}, \quad (15)$$

with coefficients

$$\alpha_s = 0.895 \times 10^{-4} H_{hf}^{(s)} \quad (16)$$

and

$$\alpha_d = \partial K(T) / \partial \chi_P^d(T) = 0.895 \times 10^{-4} H_{hf}^{(d)}.$$

¹⁸ C. H. Townes, C. Herring, and W. D. Knight, Phys. Rev. **77**, 852 (1950).

¹⁹ J. Friedel, Phil. Mag. **43**, 153 (1952); A. Blandin, E. Daniel, and J. Friedel, *ibid.* **4**, 180 (1959); A. Blandin and E. Daniel, J. Phys. Chem. Solids **10**, 126 (1959); F. J. Blatt, Phys. Rev. **108**, 285 (1957); A. M. Clogston, *ibid.* **125**, 439 (1961); J. Callaway, J. Math. Phys. **5**, 783 (1964); J. Kanamori, J. Appl. Phys. Suppl. **36**, 929 (1965); F. Gautier and P. Lengart, Phys. Rev. **139**, A705 (1965).

²⁰ A. M. Clogston, V. Jaccarino, and Y. Yafet, Phys. Rev. **134**, A650 (1964).

Here, $H_{hf}^{(s)}$ and $H_{hf}^{(d)}$ are the hyperfine fields per spin arising from the s -band and the d -band electrons, respectively. Contributions to the Knight shift from the Van Vleck type susceptibility, the diamagnetic susceptibility of the core, and the Landau diamagnetic susceptibility are temperature independent. Only the d band contributes significantly to the temperature-dependent part of the Knight shift, because the temperature variation in the density of states at the Fermi energy is smaller in the more or less flat s band compared to the peaked, narrow d band. There will also be some contribution to the temperature-dependent part of the susceptibility from the s - d exchange interaction. This contribution is usually neglected in first approximation. If the temperature variations of K and χ are large, and if K varies linearly with χ then the partial derivative [Eq. (16)] can be used to obtain the average core-polarization hyperfine field per d spin, $H_{hf}^{(d)}$.

The temperature dependence of the Knight shift expressed by Eq. (15) for a pure metal may be adapted to very *dilute* alloys of transition metals also. The Pauli-spin susceptibility from the conduction band d electrons is again the main source of the temperature-dependent part of the susceptibility. The susceptibility of the impurity is a function of the density of states at the Fermi energy (E_F). When a solute is introduced into a host metal, the density of states at the Fermi energy of the solute will be changed because of the conduction-electron scattering at the solute. The Knight shift on the solute nucleus in the host matrix is dependent on unpaired spin density at the solute nucleus. The temperature-dependent part of this spin density arises through core polarization by the d -band conduction electrons as in the pure metal. In the dilute-alloy case, however, there is an important qualification: $K_d(T)$ reflects the *local* d -spin density at the impurity atom. In Fig. 7, the Knight shift K_i , when plotted against $(T+C)^{-1}$, shows a typical Curie-Weiss behavior with $C = 321 \pm 24^\circ\text{K}$. This suggests that a large contribution to the Knight shift arises (indirectly) from the d elec-

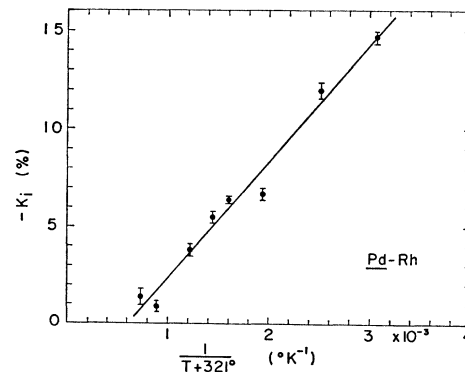


FIG. 7. Curie-Weiss behavior of the impurity Knight shift, K_i . The line represents the least-squares fit which gives $C = 321 \pm 24^\circ\text{K}$.

trons, which behave like an effective local moment with spin (S_z).

To obtain the core- d hyperfine field, $H_{\text{hf}}^{(d)}$, the impurity susceptibility was calculated from susceptibility data of Manuel and St. Quinton⁵ and of Vogt *et al.*⁶ The susceptibility of an alloy may be written as

$$\chi_{\text{alloy}} = C_i \bar{\chi}_i + C_h \bar{\chi}_h \quad (17)$$

and the "limiting impurity susceptibility" χ_i is given by

$$\chi_i = \lim_{C_i \rightarrow 0} \left(\frac{\chi_{\text{alloy}} - C_h \bar{\chi}_h}{C_i} \right), \quad (18)$$

where C_i and C_h are the number of impurity and host atoms per gram, and $\bar{\chi}_i = \partial \chi_{\text{alloy}} / \partial C_i$ and $\bar{\chi}_h = \partial \chi_{\text{alloy}} / \partial C_h$ are the impurity and the host partial susceptibilities per atom, respectively. In Fig. 8, the inverse of the calculated impurity susceptibility is plotted versus temperature. For large concentrations (curve a), the influence of impurity-impurity interactions is apparent. With decreasing concentration, the curves approach a "limiting" impurity susceptibility for zero concentration (curve g). Taking into consideration the uncertainty of the original data, curve g is compatible with a Curie-Weiss behavior with a large constant C (see Fig. 7).

In order to compare our experimental results on Knight shifts for rhodium nuclei in different host metals with theory, one would like to know the susceptibilities of the rhodium atoms alone in the host metal: These cannot be obtained with existing experimental techniques. The limiting impurity susceptibility χ_i obtained from Eq. (18) is the susceptibility contributed by the impurity to the matrix. Here, in extrapolating to $C_i = 0$ the impurity-impurity interactions are eliminated and the impurity atoms are assumed to contribute linearly to the bulk susceptibility χ_i calculated from the experimental bulk susceptibility data which contain the polarization of the Pd lattice by the rhodium atom. The Knight shifts provide, by contrast, a microscopic measurement of the electron polarization experienced by the rhodium nuclei alone.

The variations of the impurity susceptibility χ_i and the impurity Knight shift K_i with temperature are shown in Fig. 9. For comparison, the susceptibility and the Knight shift for pure palladium according to Ref. 10 are shown in the insert. Two facts should be noticed: (a) There is a striking difference, between host and impurity, of the low-temperature behavior of the Knight shift and the susceptibility, and (b) the proportionality between K and χ , observed in the host, does *not* hold for the impurity. The Knight shift for pure rhodium metal was found to vary almost linearly with temperature, decreasing by about 0.008% for an increase in temperature by about 100°K.⁴ The Knight shifts on palladium nuclei in palladium metal follow the familiar susceptibility curve, with a broad maximum

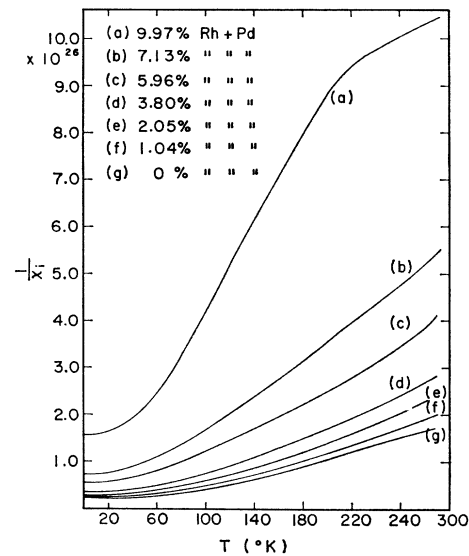


Fig. 8. Inverse of the impurity susceptibility, $1/\chi_i$, plotted as a function of temperature for different concentrations of rhodium. The impurity susceptibility values were calculated from the experimental data of Manuel and Quinton (see Ref. 5). Curve (g) was obtained by extrapolation to zero concentration.

around 85°K. The decrease in the Knight shift immediately above 85°K is roughly 0.7% for an increase of 100°K.¹⁰ The impurity Knight shift (K_i) for rhodium in palladium, plotted in Fig. 9, has a much stronger temperature dependence. The impurity Knight shift of rhodium in palladium does not follow the host lattice. We interpret this fact together with the Curie-Weiss behavior of the Knight shift as arising from the *formation of localized moments on the impurity rhodium atom in the host matrix of palladium*. It was suggested by Jaccarino, Walker, and Wertheim²¹ that localized magnetic moments of impurities in ferromagnetic transition series hosts may sometimes be recognized by a departure of the temperature dependence of H_{hf} for the impurity from that of the host. Experimental NMR data for Mn in Fe²² and PAC data for ⁹⁹Ru in Ni²³ support this result. The present work is an example of the analogous situation in a nonferromagnetic host. There are several such examples, although all, to our knowledge, involve "magnetic" solutes.

The experimental values of the impurity Knight shifts ($-K_i/\%$) plotted against the limiting impurity susceptibility χ_i , with temperature as the implicit parameter, are given in Fig. 10. The data show a striking break about the χ_i value corresponding to a temperature of about 400°K. The break indicates the occurrence of two very different core- d hyperfine fields below and

²¹ V. Jaccarino, J. R. Walker, and G. K. Wertheim, Phys. Rev. Letters **13**, 752 (1964).

²² Y. Koi, A. Tsujimura, and T. Hihara, J. Phys. Soc. Japan **19**, 1493 (1964).

²³ D. A. Shirley, S. S. Rosenblum, and E. Matthias, Phys. Rev. **170**, 363 (1968).

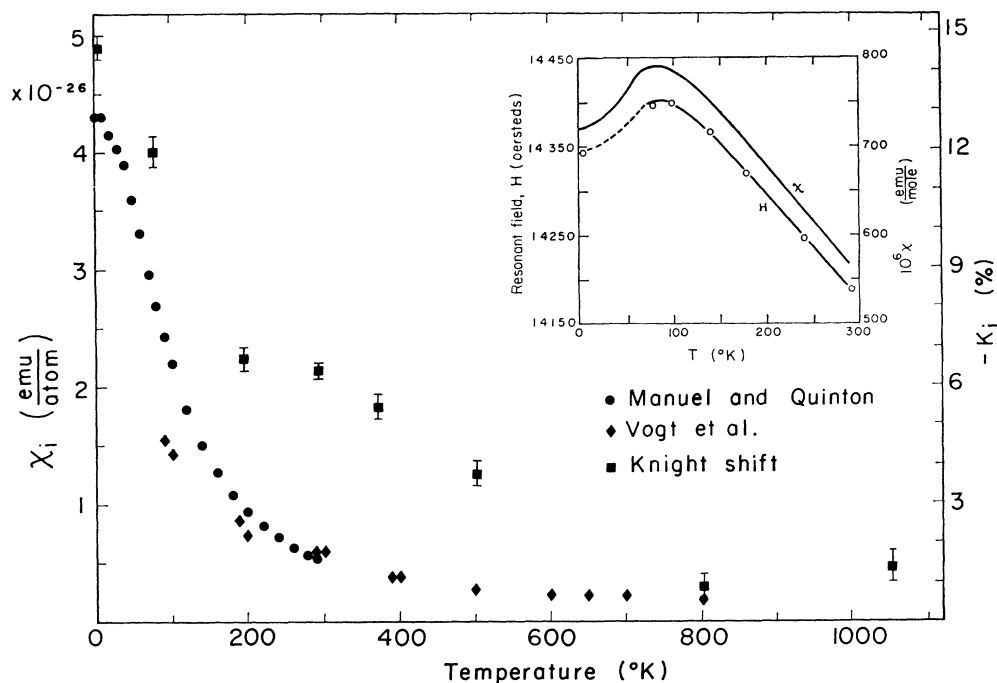


FIG. 9. The impurity Knight shift (K_i) and the impurity susceptibility χ_i for zero concentration of rhodium plotted against temperature. The impurity susceptibility values were calculated by extrapolating the data of Manuel and Quinton (see Ref. 5) and Vogt *et al.* (see Ref. 6). For comparison, the Knight shift and susceptibility versus temperature for pure palladium (see Ref. 10) is shown in the insert.

bove this temperature. A fit of all points with $-K_i > 5\%$ corresponding to temperatures $T \leq 400^\circ\text{C}$ yields a value of $H_{\text{hf}}^{(d)} = -43 \pm 1$ kG. There are not enough high-temperature data available to permit a reliable fit to a straight line. The dashed line corresponds to a core- d hyperfine field of $H_{\text{hf}}^{(d)} = -700$ kG: It approximates the high-temperature slope fairly well.

A summary of core- d hyperfine fields for rhodium and palladium is given in Table IV. Seitchik *et al.*⁴ measured

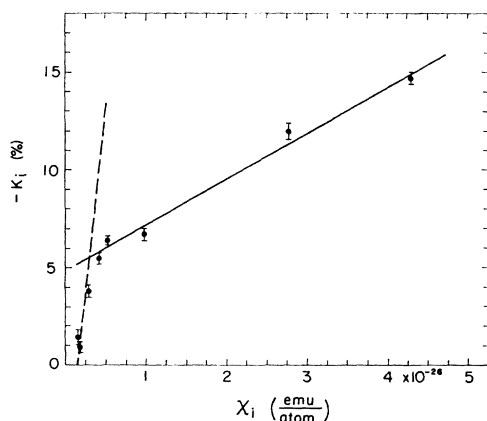


FIG. 10. Impurity Knight shifts plotted versus zero-concentration impurity susceptibility, with temperature as an implicit parameter. The solid line represents the fit to all points with $T \leq 400^\circ\text{K}$. The dashed line indicates the slope that would correspond to a core- d hyperfine field of $H_{\text{hf}}^{(d)} = -700$ kG/spin.

the temperature dependence of the Knight shift for pure rhodium metal using conventional NMR. From $\partial K(T)/\partial \chi(T)$, they obtain the average core-polarization hyperfine field $H_{\text{hf}}^{(d)} = -323$ kG/spin for rhodium nuclei in pure rhodium metal. Similar studies¹⁰ by the same group gave the average core-polarization hyperfine field $H_{\text{hf}}^{(d)} = -689 \pm 20$ kG/spin for palladium nuclei in palladium metal. Using the exchange-polarized Hartree-Fock method, Freeman²⁴ calculated the core-polarization hyperfine fields in $4d$ ions. His values for $\text{Pd}^{2+}(4d)^8$ and $\text{Pd}^{3+}(4d)^7$ are -749 and -726 kG/spin, respectively. Freeman's calculations also show that in $4d$ ions there is no conspicuous variation in the average core-polarization hyperfine fields with atomic number. The core-polarization hyperfine field experimentally obtained for palladium nuclei in palladium metal¹⁰ is in good agreement with the theoretical calculations of Freeman. The large variation in the core-polarization hyperfine fields from rhodium to palladium obtained by the Bell Laboratories group is rather unexpected. However, there are no exhaustive experimental studies of the average core-polarization hyperfine fields in $4d$ transition metals as a function of the atomic number. $3-d$ shell paramagnetic ions in non-metallic crystals do not show abrupt variations in the

²⁴ A. J. Freeman, in *Hyperfine Structure and Nuclear Radiations*, edited by E. Matthias and D. A. Shirley (North-Holland Publishing Co., Amsterdam, 1968), p. 427.

TABLE IV. Comparison of the core-polarization hyperfine fields.

Reference	Method	Details	Core-polarization hyperfine field per d spin
Freeman (Ref. 24)	a	$\left\{ \begin{array}{l} \text{Pd}^{2+}(4d)^8 \\ \text{Pd}^{2+}(4d)^7 \end{array} \right.$	$H_{\text{hf}}^{(d)} = -726$ kG/spin $H_{\text{hf}}^{(d)} = -749$ kG/spin
Seitchik <i>et al.</i> (Ref. 4)	b	Rh in Rh	$H_{\text{hf}}^{(d)} = -323$ kG/spin
Seitchik <i>et al.</i> (Ref. 10)	b	Pd in Pd	$H_{\text{hf}}^{(d)} = -689(20)$ kG/spin
Present measurements	c	dilute Rh in Pd	$\left\{ \begin{array}{l} T < 400^\circ\text{K}: H_{\text{op}} = -43 \text{ kG/spin} \\ T > 400^\circ\text{K}: H_{\text{op}} \approx -700 \text{ kG/spin} \end{array} \right.$

^a Exchange-polarized Hartree-Fock calculations.

^b Temperature dependence of the Knight shift using NMR.

^c Temperature dependence of the Knight shift using DAPAC.

measured core-polarization hyperfine fields as a function of atomic number.

From Fig. 10, we must conclude that the localized moment at the rhodium atom changes its character at about 400°K. Above this temperature, a core-polarization hyperfine field of about -700 kG/spin is present, in agreement with theoretical predictions²⁴ and other results.¹⁰ Below this temperature the value of $H_{\text{hf}}^{(d)}$ drops sharply, and we find that *only a small fraction of the total electron polarization* arising from the rhodium solute atom is concentrated on that atom. If we compare the result of $H_{\text{hf}}^{(d)} = -43$ kG with the result of Seitchik *et al.*⁴ for rhodium metal, we find that less than 13% of the polarization is concentrated on the rhodium nucleus and the remaining 87% of the polarization is elsewhere in the matrix. This conclusion is only strengthened if it is referred to a core-polarization hyperfine field of about -700 kG/spin²⁴ in the 4d ions. In either case, we conclude that the polarization of the matrix from the impurity rhodium atom below 400°K is comparatively long range, extending over at least several neighbors.

It is difficult to assess the accuracy of χ_i ; for this reason and because of the lack of other data on the Rh-Pd system, we are reluctant to make an extensive interpretation of these results. It seems clear, however, that localized moments are formed on Rh atoms in

Pd. At low temperatures, a quasibound (Kondo) state seems to be formed between the local moment and conduction electrons. Klein has shown,²⁵ using the theory of Takano and Ogawa,²⁶ that s - d interaction in a Kondo state below the transition temperature T_K should give a positive contribution to the Knight shift at an impurity. Both this effect and an increase below T_K of the total spin polarization of the lattice induced by the local moment would lead to the behavior illustrated in Fig. 10. While this is an attractive interpretation, further supporting evidence will be required before it can be regarded as firm.

ACKNOWLEDGMENTS

One of us (GNR) is grateful to Professor John O. Rasmussen for his kind interest and encouragement. We are thankful to Dr. Albert Narath and Professor S. Foner for sending their susceptibility data prior to publication, and to Professor Alan P. Klein for communicating his calculations prior to publication. We also express our sincere thanks to Mrs. Wini Heppler for numerous skillful and dependable radioactive chemical separations.

²⁵ A. P. Klein, Phys. Rev. **181**, 579 (1969).

²⁶ F. Takano and T. Ogawa, Progr. Theoret. Phys. (Kyoto) **35**, 343 (1966).